

Investigation of the Transformation Between Differential-Mode and Common-Mode Noises in an EMI Filter Due to Unbalance

Shuo Wang, *Senior Member, IEEE*, and Fred C. Lee, *Fellow, IEEE*

Abstract—This paper analyzes the transformation between differential-mode and common-mode noises due to the unbalance of noise sources and electromagnetic interference filters in power electronics circuits. Both insertion gain and electromagnetic interference measurements prove the analysis.

Index Terms—Electromagnetic interference (EMI) filter, mode transformation, unbalance.

I. INTRODUCTION

IN POWER electronics systems, the switching-mode power supply generates significant electromagnetic interference (EMI) noise. EMI filters are used to suppress EMI noise. In order to efficiently analyze and design EMI filters, the filters are usually decoupled into differential-mode (DM) and common-mode (CM) filters [4], [5], [7]. The DM and CM attenuation of the filters can then be analyzed, respectively [5]. This decoupling is based on the assumption that EMI filters have perfectly symmetric circuit structures. For the typical EMI filter shown in Fig. 1, two CM windings are coupled, and the CM inductances of the two windings are L_{CM1} and L_{CM2} . The DM inductances L_{DM1} and L_{DM2} are the leakage inductances of the two coupled CM windings. C_1 and C_2 are DM capacitors, and C_{Y1} and C_{Y2} are CM capacitors. It is assumed that L_{CM1} equals L_{CM2} , C_{Y1} equals C_{Y2} , and L_{DM1} equals L_{DM2} . The printed circuit board (PCB) layout is also perfectly symmetric. As a result, CM current would not flow through DM capacitors C_1 and C_2 , and the DM noise voltage potential on the centerline is zero. The EMI filters can then be decoupled into a CM filter and a DM filter, as shown in Fig. 2.

For this decoupling approach, it is assumed that DM and CM noises are independent of each other, so the DM and CM attenuations of the filter can be evaluated separately. In a practical case, strictly speaking, component parameters such as L_{CM1} and L_{CM2} , C_{Y1} and C_{Y2} , and L_{DM1} and L_{DM2} are not perfectly equal, so DM and CM filters cannot be totally decoupled, as shown in Fig. 2. DM noise can transform into CM noise and *vice versa* due to these asymmetries. Two more general

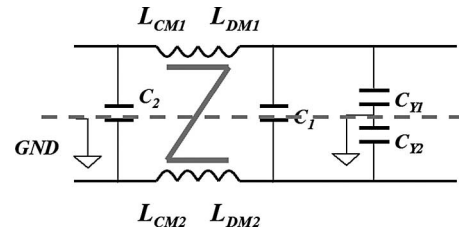


Fig. 1. EMI filter with balanced circuit structure.

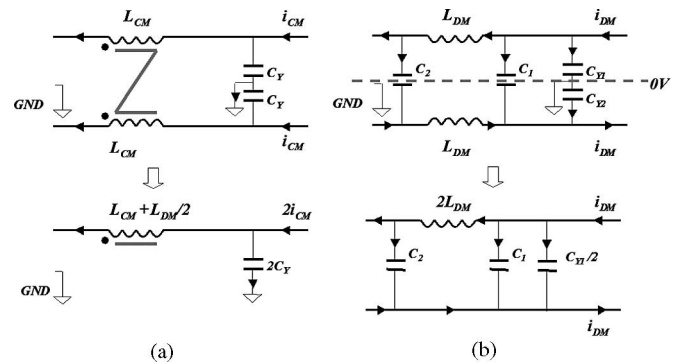


Fig. 2. Decoupling EMI filters into CM and DM filters. (a) CM filter and its equivalent circuit. (b) DM filter and its equivalent circuit.

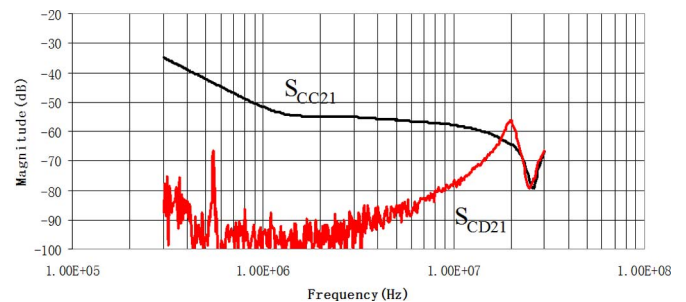


Fig. 3. Comparison of measured S_{CD21} and S_{CC21} .

concepts used to describe the transformation between CM and DM noises are balance and unbalance. Fig. 3 shows a measured transmission coefficient S_{CD21} (mixed-mode S parameter) [2], [10] with DM excitation and CM response. It is compared with the measured S_{CC21} with CM excitation and CM response. The measurement is carried out using an Agilent E5070B four-port balanced RF network analyzer [1].

Fig. 3 shows that S_{CD21} is as high as S_{CC21} above 22 MHz and even higher around 20 MHz. This could be a problem for noise attenuation. For example, before the EMI filter is applied,

Manuscript received June 14, 2009; revised October 28, 2009; accepted November 30, 2009. Date of publication February 5, 2010; date of current version August 18, 2010.

S. Wang is with the Electrical Power Systems, GE Aviation Systems, Vandalia, OH 45377 USA (e-mail: shuowang@ieee.org).

F. C. Lee is with the Center for Power Electronics Systems, Virginia Polytechnic Institute and State University, Blacksburg, VA 24061 USA (e-mail: fcllee@vt.edu).

Color versions of one or more of the figures in this paper are available online at <http://ieeexplore.ieee.org>.

Digital Object Identifier 10.1109/TEMC.2009.2038899

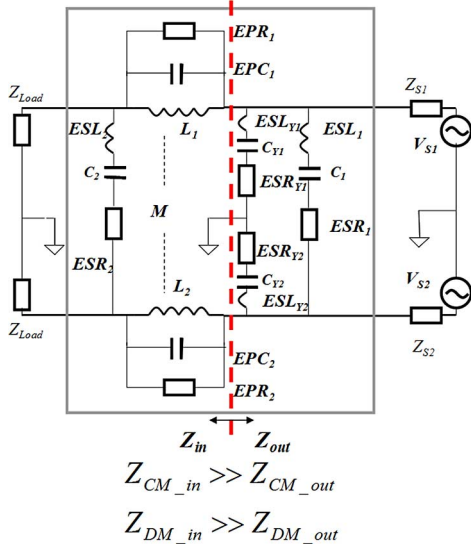


Fig. 4. EMI filter including parasitic parameters.

at 20 MHz, the DM noise is $120 \text{ dB} \cdot \mu\text{V}$ and the CM noise is $100 \text{ dB} \cdot \mu\text{V}$. After the filter is connected to the circuit, the CM noise is attenuated to $37 \text{ dB} \cdot \mu\text{V}$ by the CM filter. At the same time, the CM noise that is transformed from the DM noise is $63 \text{ dB} \cdot \mu\text{V}$, which is much higher than the attenuated CM noise. This could make filter design inefficient, since mode transformation is not expected in the original EMI filter design. The traditional decoupling method for CM and DM signal analysis is difficult to be applied to this case because the DM and CM noises are coupled together due to unbalance. For example, in Fig. 1, if C_{Y1} and C_{Y2} are not exactly the same, part of the CM noise would transform to DM noise in these two CM capacitors. The transformed DM noise would then be attenuated by the DM inductor and the DM capacitor C_2 . The noise generated by CM excitation therefore partly flows through the CM filter and the DM filter. In the traditional decoupling method, the CM noise is supposed to flow through the CM filter only and the DM noise is supposed to flow through the DM filter only, so it cannot give the correct results.

It is necessary to explore and understand the effects of unbalance on EMI filter performance so as to efficiently design EMI filters for power electronics systems. The effects of the unbalance on system EMI are explored in [8]. This paper analyzes the mode transformation between DM and CM noises in an EMI filter caused by the unbalanced parameters. Experiments are carried out to verify the analysis. The theory developed here can also be applied to system analysis.

II. ANALYSIS OF MODE TRANSFORMATION

Not all components in EMI filters cause mode transformation between CM and DM noises. The parasitic model of the filter shown in Fig. 1 is shown in Fig. 4. The parasitics include the equivalent series inductance (ESL) and the equivalent series resistance (ESR) of the capacitors, and the equivalent parallel winding capacitance (EPC) and equivalent parallel resistance (EPR) of the inductors in the EMI filter. In

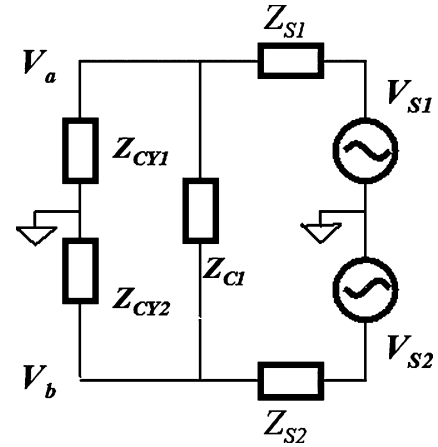


Fig. 5. Representing the right-hand side of Fig. 4 using impedances.

Fig. 4, DM capacitors C_1 and C_2 are across two lines, so there are no balance issues. As a result, they would not cause mode transformation. Instead, DM inductors L_{DM1} and L_{DM2} , CM inductors L_{CM1} and L_{CM2} , and CM capacitors C_{Y1} and C_{Y2} can cause mode transformation.

At high frequencies, parasitics of the components determine their performance, so the unbalance of parasitics determines the mode transformation. The equivalent parallel winding capacitances EPC_1 and EPC_2 of the inductors and the equivalent series inductances ESL_{Y1} and ESL_{Y2} of the capacitors would cause mode transformation. This paper ignores the effects of the parasitic mutual couplings between the components on mode transformation in analysis. This paper ignores the effects of M_3 , the parasitic mutual inductance between two DM capacitors, on the DM insertion gain are discussed later. For the general case shown in Fig. 4, the load of the EMI filters is power lines terminated by two balanced LISNs, and the source of the EMI filters is an unbalanced converter.

A. Partition of the Filter

In the interface, which is defined by the dashed line in Fig. 4, the output impedance Z_{out} on the right-hand side is much smaller than the input impedance Z_{in} on the left-hand side within the concerned frequency range. This results from the mismatch rule in EMI filter design [6]. The EMI filter can be split into two mismatched networks. For the right-hand side, the circuit is represented by Fig. 5 using impedances on every branch. On the left-hand side, DM inductors L_{DM1} and L_{DM2} are not coupled, since they are the leakage of CM inductors L_{CM1} and L_{CM2} . CM inductors L_{CM1} and L_{CM2} are closely coupled at frequencies before the parallel resonant frequency of L_{CM} and EPC. After the resonant frequency, most of the CM noise will flow through EPC instead of L_{CM} . The coupled inductor can be decoupled as shown in Fig. 6. After the inductors are decoupled, all components on the left-hand side are no longer coupled. The components on the left-hand side of Fig. 4 can then be replaced by Fig. 7 using impedances on every branch.

Because the noise sources are unbalanced, the excitations shown in Fig. 5 are composed of both DM excitation \tilde{V}_D and

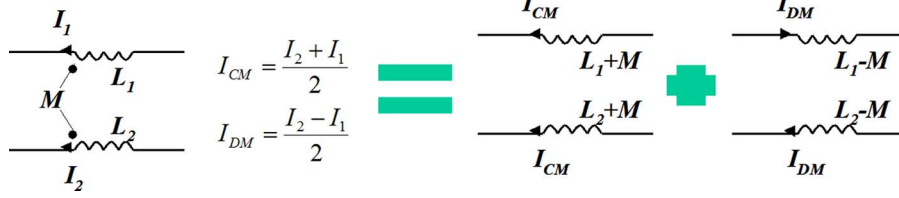


Fig. 6. Decoupling DM and CM inductors.

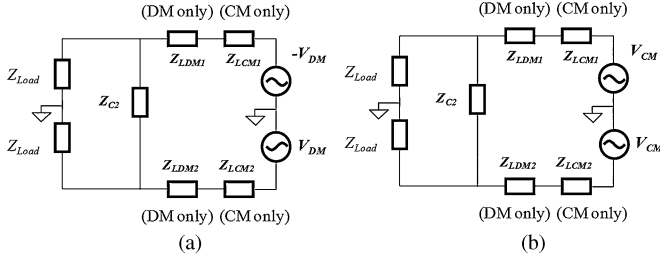


Fig. 7. Representing the left-hand side of Fig. 4 using impedances. (a) DM excitation. (b) CM excitation.

CM excitation \tilde{V}_C , which are given by (1) and (2), respectively. The outputs of the right-hand side are \tilde{V}_a and \tilde{V}_b , which can be represented using the DM response \tilde{V}_{DM} and CM response \tilde{V}_{CM} . These are given by (3) and (4). \tilde{V}_{DM} and \tilde{V}_{CM} then work as the excitations on the left-hand side of Fig. 4, as shown in Fig. 7. The output impedances on the right-hand side are ignored in Fig. 7 since they are much smaller than the input impedances on the left-hand side within the concerned frequency range.

$$\tilde{V}_D = \frac{\tilde{V}_{S2} - \tilde{V}_{S1}}{2} \quad (1)$$

$$\tilde{V}_C = \frac{\tilde{V}_{S2} + \tilde{V}_{S1}}{2} \quad (2)$$

$$\tilde{V}_{DM} = \frac{\tilde{V}_b - \tilde{V}_a}{2} \quad (3)$$

$$\tilde{V}_{CM} = \frac{\tilde{V}_b + \tilde{V}_a}{2}. \quad (4)$$

B. Analysis of DM Excitation

It is well known that any two impedances can be expressed by the sum or difference of their impedance average and impedance difference. The larger impedance of the two is equal to the sum of the average and half of the difference. The smaller one is equal to the difference between the average and half of the difference. The ratio of the impedance difference to impedance average can be used to represent impedance unbalance in an EMI filter. It represents how much one of the impedances deviates from their average. The impedance difference and the impedance average of the noise source, CM capacitors, and DM and CM inductors are defined in (5), (7), (9), and (11).

One advantage of defining two impedances with their impedance difference and impedance average in the following analysis is that high-order terms (products of impedance differences) can be ignored so that the analysis can be greatly

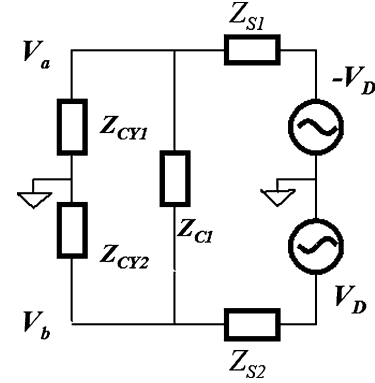


Fig. 8. DM excitation on the right-hand side of Fig. 4.

simplified. Furthermore, the effects of unbalance are very straightforward when they are directly expressed by unbalance.

The noise source impedances Z_{S1} and Z_{S2} , the impedances of the CM capacitors Z_{CY1} and Z_{CY2} , the impedances of the CM inductors Z_{LCM1} and Z_{LCM2} , and the impedance of DM inductors Z_{LDM1} and Z_{LDM2} can then be expressed using their impedance average and impedance difference in (6), (8), (10), and (12), respectively, as

$$\Delta Z_S = \frac{Z_{S2} - Z_{S1}}{2} \quad Z_S = \frac{Z_{S2} + Z_{S1}}{2} \quad (5)$$

$$Z_{S1} = Z_S - \Delta Z_S \quad Z_{S2} = Z_S + \Delta Z_S \quad (6)$$

$$\Delta Z_{CY} = \frac{Z_{CY2} - Z_{CY1}}{2} \quad Z_{CY} = \frac{Z_{CY2} + Z_{CY1}}{2} \quad (7)$$

$$Z_{CY1} = Z_{CY} - \Delta Z_{CY} \quad Z_{CY2} = Z_{CY} + \Delta Z_{CY} \quad (8)$$

$$\Delta Z_{LDM} = \frac{Z_{LDM2} - Z_{LDM1}}{2} \quad Z_{LDM} = \frac{Z_{LDM2} + Z_{LDM1}}{2} \quad (9)$$

$$Z_{LDM1} = Z_{LDM} - \Delta Z_{LDM} \quad Z_{LDM2} = Z_{LDM} + \Delta Z_{LDM} \quad (10)$$

$$\Delta Z_{LCM} = \frac{Z_{LCM2} - Z_{LCM1}}{2} \quad Z_{LCM} = \frac{Z_{LCM2} + Z_{LCM1}}{2} \quad (11)$$

$$Z_{LCM1} = Z_{LCM} - \Delta Z_{LCM} \quad Z_{LCM2} = Z_{LCM} + \Delta Z_{LCM}. \quad (12)$$

As stated before, the noise excitations are decoupled into DM and CM in (1) and (2). For the DM excitation shown in Fig. 8, the DM and CM responses defined in (3) and (4) can be calculated by solving network equations. Ignoring all second-order terms,

the final results are given in (13)–(15), shown at the bottom of the page.

The attenuation on DM noise is given by (13). The transformation from DM to CM noise is given by (14). As stated in previous part, the unbalance is represented with the ratio of impedance difference to impedance average in (14). These equations show that the transformation has a linear relationship with the unbalance. From (5) and (7), ΔZ_S and ΔZ_{CY} can be positive and negative, so the total effect of the unbalances would be the sum or difference of the effects of the two unbalances. From (15), even if Z_{C1} is zero, the transformation still cannot be eliminated; thus, the effects of the unbalanced DM noise source cannot be eliminated by using a DM capacitor to balance two lines. The reason behind this is that the transformation from DM to CM due to the unbalance, of DM source impedances results in CM noise on C_{Y1} , C_{Y2} , and C_1 , where C_1 is a DM capacitor, so it cannot eliminate the transformed CM noise.

The DM and CM responses of the right-hand side act as DM and CM excitations of the left-hand side, which is shown in Fig. 7. The final CM and DM responses on loads due to these two excitations are given by

$$\tilde{V}_{\text{LoadCM}} = \frac{Z_{\text{Load}}}{(Z_{\text{LCM}} + Z_{\text{Load}})} \left(\tilde{V}_{\text{CM}} - \frac{\Delta Z_{\text{LDM}}}{Z_{\text{LDM}}} \tilde{V}_{\text{DM}} \right) \quad (16)$$

$$\tilde{V}_{\text{LoadDM}} = \frac{Z_{C2}}{2Z_{\text{LDM}}} \left(\tilde{V}_{\text{DM}} - \frac{\Delta Z_{\text{LCM}}}{(Z_{\text{LCM}} + Z_{\text{Load}})} \tilde{V}_{\text{CM}} \right). \quad (17)$$

Substituting (13) and (14) into (16) and (17) and ignoring all second-order terms, the final expressions for DM and CM responses are given by

$$\tilde{V}_{\text{LoadDM}} \approx k_D \tilde{V}_D \quad (18)$$

$$\tilde{V}_{\text{LoadCM}} \approx \left[-k_1 \frac{\Delta Z_S}{Z_S} + k_2 \frac{\Delta Z_{CY}}{Z_{CY}} - k_3 \frac{\Delta Z_{\text{LDM}}}{Z_{\text{LDM}}} \right] \tilde{V}_D \quad (19)$$

$$k_D = \frac{Z_{C2}}{2Z_{\text{LDM}} Z_S} \frac{1}{1/(Z_{C1}/2) + 1/Z_S + 1/Z_{CY}} \quad (20)$$

$$k_3 = \frac{Z_{\text{Load}}}{(Z_{\text{LCM}} + Z_{\text{Load}}) Z_S} \frac{1}{[1/(Z_{C1}/2) + 1/Z_S + 1/Z_{CY}]} \quad (21)$$

$$k_2 = \frac{1}{(1 + Z_{CY}/Z_S)} k_3 \quad (22)$$

$$k_1 = \frac{1/(Z_{C1}/2) + 1/Z_{CY}}{(1/Z_{CY} + 1/Z_S)} k_3 = \left(1 + \frac{2Z_{CY}}{Z_{C1}} \right) k_2. \quad (23)$$

These equations show that the CM response due to the unbalanced parameters is composed of three parts. The first part is due

to the unbalanced noise source impedances, the second part is due to the unbalanced impedances of CM capacitors, and the last part is due to the unbalanced impedances of DM inductors. The mode transformation has a linear relationship with these three unbalances because they are small so that higher order terms can be ignored. In the mode transformation equation in (18), the unbalances on the power delivery paths lead to negative coefficients, and those on shunt paths lead to positive coefficients. From (19), theoretically, it is possible to adjust three single unbalances to achieve a balance as a whole in certain frequency ranges.

Since k_1 , k_2 , and k_3 are not functions of Z_{C2} , the DM capacitor in the output loop does not help suppress the CM noise transformed from DM noise. It has been analyzed previously that Z_{C1} cannot eliminate the CM noise transformed from DM noise if the noise source is unbalanced. For the similar reason, C_2 cannot eliminate the transformation due to the unbalance of L_{DM} , C_Y , and Z_S . Because of these, DM capacitors cannot eliminate the CM noise transformed from DM noise due to unbalance. Furthermore, for CM noise, load and CM inductor achieve only -20dB/dec attenuation at the output; on the contrary, DM inductor and DM capacitor C_2 can achieve -40 dB/dec attenuation at the output. This also makes it difficult to suppress the transformed CM noise from DM noise.

C. Analysis of CM Excitation

The right-hand side of Fig. 4 with the CM excitation is shown in Fig. 9. Using the same definitions as (5)–(12), the DM and CM responses defined in (3) and (4), respectively, are calculated by solving network equations. Ignoring all second-order terms, the final results are given by

$$\tilde{V}_{\text{CM}} \approx \frac{Z_{CY}}{Z_{CY} + Z_S} \tilde{V}_C \quad (24)$$

$$\tilde{V}_{\text{DM}} \approx \frac{\tilde{V}_C}{(Z_S + Z_{CY}) [1/(Z_{C1}/2) + 1/Z_S + 1/Z_{CY}]} \times \left(\frac{\Delta Z_{CY}}{Z_{CY}} - \frac{\Delta Z_S}{Z_S} \right) \quad (25)$$

$$Z_{C1} \rightarrow 0 \Rightarrow \tilde{V}_{\text{DM}} \rightarrow 0. \quad (26)$$

The transformation from CM to DM is composed of two parts. The first part is due to the unbalanced CM capacitor and the second part is due to the unbalanced noise source impedances. Once again, based on (5) and (7), ΔZ_S and ΔZ_{CY} can be positive and negative, so the total effects of the unbalances would be the sum or difference of the effects of the two unbalances. Theoretically,

$$\tilde{V}_{\text{DM}} \approx \frac{\tilde{V}_D}{Z_S} \frac{1}{1/(Z_{C1}/2) + 1/Z_S + 1/Z_{CY}} \quad (13)$$

$$\tilde{V}_{\text{CM}} \approx \frac{\tilde{V}_D}{(Z_S + Z_{CY})} \left\{ \frac{\Delta Z_{CY}}{Z_{CY}} \frac{1}{[1/(Z_{C1}/2) + 1/Z_S + 1/Z_{CY}]} - \frac{\Delta Z_S}{Z_S} Z_{CY} \left[1 - \frac{1}{Z_S [1/(Z_{C1}/2) + 1/Z_S + 1/Z_{CY}]} \right] \right\} \quad (14)$$

$$Z_{C1} \rightarrow 0 \Rightarrow \tilde{V}_{\text{CM}} \rightarrow -\frac{Z_{CY} \tilde{V}_D}{(Z_S + Z_{CY})} \frac{\Delta Z_S}{Z_S} \quad (15)$$

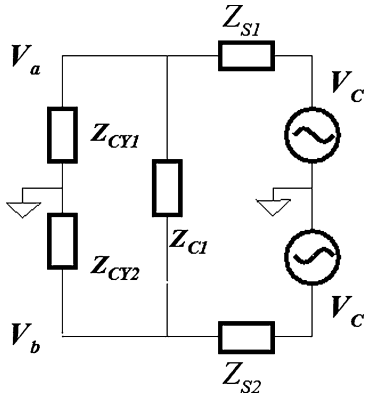


Fig. 9. CM excitation on right-hand side of Fig. 4.

by adjusting these two unbalances, it is possible to achieve a balance as a whole. From (25), if Z_{C1} is an infinitely large DM capacitance, whose impedance is zero, the mode transformation from CM to DM can be eliminated. Compared with the transformation from DM to CM described in (14) and (15), the story is different since a large DM capacitance cannot eliminate the transformation from DM to CM due to the unbalance of noise sources. Because of this, the transformation from DM to CM is more significant than that from CM to DM for the filter shown in Fig. 1.

The DM and CM responses of the right-hand side act as the excitations of the left-hand side shown in Fig. 7. The final responses are still given by (16) and (17). Substituting (24) and (25) into (16) and (17) and ignoring all second-order terms, the final expressions for DM and CM responses are given by

$$\tilde{V}_{\text{LoadCM}} \approx k_C \tilde{V}_C \quad (27)$$

$$\tilde{V}_{\text{LoadDM}} = \left[-k_5 \frac{\Delta Z_S}{Z_S + Z_{CY}} + k_6 \frac{\Delta Z_{CY}}{Z_S + Z_{CY}} - k_7 \frac{\Delta Z_{LDM}}{Z_{LDM} + Z_{\text{Load}}} \right] \tilde{V}_C \quad (28)$$

$$k_C = \frac{Z_{\text{Load}} Z_{CY}}{(Z_{LDM} + Z_{\text{Load}})(Z_S + Z_{CY})} \quad (29)$$

$$k_5 = \frac{Z_{C2}}{2Z_{LDM} Z_S} \frac{1}{[1/(Z_{C1}/2) + 1/Z_S + 1/Z_{CY}]} = \frac{Z_{CY}}{Z_S} k_6 \quad (30)$$

$$k_6 = \frac{Z_{C2}}{2Z_{LDM} Z_{CY}} \frac{1}{[1/(Z_{C1}/2) + 1/Z_S + 1/Z_{CY}]} \quad (31)$$

$$k_7 = \frac{Z_{C2} Z_{CY}}{2Z_{LDM} (Z_S + Z_{CY})}. \quad (32)$$

These equations show that the DM response due to unbalances is composed of three parts. The first part is due to the unbalanced noise source impedances, the second part is due to the unbalanced impedance of CM capacitors, and the last part is due to the unbalanced impedances of inductors. The mode transformation has a linear relationship with these unbalances. In the mode transformation equation (28), the unbalances on the power delivery paths lead to negative coefficients and

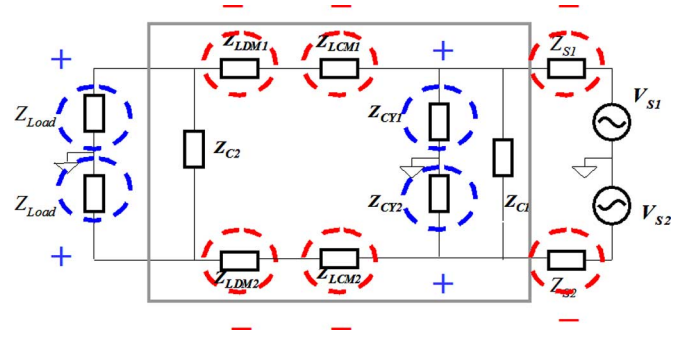


Fig. 10. Effects of unbalance on EMI filter performance.

those on shunt paths lead to positive coefficients. When DM capacitors C_2 or C_1 has a very low impedance, k_5 – k_7 are close to zero, so the DM capacitors can efficiently reduce the DM noise transformed from the CM noise. This is different from the transformation from DM to CM. Because of this, the mode transformation from DM to CM is prone to be more significant than that from CM to DM

$$\begin{aligned} \tilde{V}_{\text{LoadDM}} &= \left[-k_5 \frac{\Delta Z_S}{Z_S + Z_{CY}} + k_6 \frac{\Delta Z_{CY}}{Z_S + Z_{CY}} - k_7 \frac{\Delta Z_{LDM}}{Z_{LDM} + Z_{\text{Load}}} \right. \\ &\quad \left. + \left(-k_9 \frac{\Delta Z_S}{Z_S + Z_{CY}} + k_{10} \frac{\Delta Z_{CY}}{Z_S + Z_{CY}} \right) Z_{M3} \right] \tilde{V}_C \end{aligned} \quad (33)$$

$$Z_{M3} = j\omega M_3 \quad (34)$$

$$k_9 = \frac{2}{Z_S Z_{C1}} \frac{1}{[1/(Z_{C1}/2) + 1/Z_S + 1/Z_{CY}]} \quad (35)$$

$$k_{10} = \frac{2}{Z_{CY} Z_{C1}} \frac{1}{[1/(Z_{C1}/2) + 1/Z_S + 1/Z_{CY}]} \quad (36)$$

If the parasitic mutual coupling between two DM capacitors is considered, (28) can be rewritten as (33)–(36). Z_{M3} is the impedance of mutual inductance M_3 between two DM capacitors, as defined in (34). M_3 does not affect the propagation of CM noise. The unbalanced mutual couplings between inductors and capacitors, between noise source and filter components will also contribute to mode transformations, however, they are not analyzed here.

D. Summary of the Effects of Unbalances

For the general case shown in Fig. 10, the general expressions for mode transformation due to unbalances are shown in (37) and (38). If the mutual coupling between the two DM capacitors is considered, two more terms as in (33) should be included in the following equations:

$$\begin{aligned} \tilde{V}_{\text{LoadCM}} &\approx \left[-k_1 \frac{\Delta Z_S}{Z_S} + k_2 \frac{\Delta Z_{CY}}{Z_{CY}} - k_3 \frac{\Delta Z_{LDM}}{Z_{LDM}} \right. \\ &\quad \left. + k_4 \frac{\Delta Z_{\text{Load}}}{Z_{\text{Load}}} \right] \tilde{V}_D \end{aligned} \quad (37)$$

$$\tilde{V}_{\text{LoadDM}} \approx \begin{bmatrix} -k_5 \frac{\Delta Z_S}{(Z_S + Z_{CY})} + k_6 \frac{\Delta Z_{CY}}{(Z_S + Z_{CY})} \\ -k_7 \frac{\Delta Z_{LCM}}{(Z_{LCM} + Z_{Load})} + k_8 \frac{\Delta Z_{Load}}{(Z_{LCM} + Z_{Load})} \end{bmatrix} \tilde{V}_C. \quad (38)$$

If more stages are cascaded and each stage meets the impedance mismatch conditions, the general expression for mode transformations can be given by

$$\tilde{V}_{\text{LoadCM}} \approx \left[\sum_{n=1}^m k_n \frac{\Delta Z_n}{Z_n} - \sum_{p=1}^q k_p \frac{\Delta Z_p}{Z_p} \right] \tilde{V}_D \quad (39)$$

$$\tilde{V}_{\text{LoadDM}} \approx \left[\sum_{n=1}^{m,q} \frac{k_n \Delta Z_n - k_p \Delta Z_p}{Z_n + Z_p} \right] \tilde{V}_C \quad (40)$$

where m is the number of stages on power delivery path, Z_n is the impedance on the power delivery path of each stage, ΔZ_n is impedance difference, k_n is its coefficient, q is the number of shunt CM capacitor pairs, Z_p is the impedance on the shunt path for each stage, ΔZ_p is impedance difference, and k_p is its coefficient. $Z_n + Z_p$ is actually the impedance of the CM path. The effects of these unbalances on mode transformation depend on both the unbalances and their coefficients. From (39) and (40), theoretically, it is possible to adjust unbalances to achieve a balance as a whole. The DM capacitors can improve more on the suppression of mode transformation from CM to DM than that from DM to CM.

III. EXPERIMENTS

In the experiment, a one-stage EMI filter is investigated. Both source and load impedances are balanced, which is achieved by an Agilent E5070B network analyzer [1]. The practical CM capacitors and filter inductors, which cannot be perfectly balanced, are measured using precision impedance analyzer HP4294A.

The capacitor's R - L - C series equivalent circuits are derived from the measured curve. For C_{Y1} , they are 74 m Ω , 9.96 nH, and 6.9 nF. For C_{Y2} , they are 66.8 m Ω , 9.8 nH, and 7.54 nF.

Two DM capacitors are also measured and R - L - C series equivalent circuits are derived.

C1: ESR₁ is 35.3 m Ω , ESL₁ is 17.4 nH, and C_1 is 475 nF.

C2: ESR₂ is 34.9 m Ω , ESL₂ is 16.2 nH, and C_2 is 492 nF.

For the inductor, a toroidal core OJ42908TC (Magnetics) is used. Two windings, each a 21-turn AWG20, are wound on each side. Although the two windings have the same number of turns and are symmetrically located on the two sides of the core, two CM winding's parameters are still a little bit different. The measured parameters for the R - L - C parallel equivalent circuit are as follows.

Winding 1: L_{CM1} 3.09 mH, EPC₁ 8.14 pF, and EPR₁ 14.42 k Ω .

Winding 2: L_{CM2} 3.1 mH, EPC₂ 6.23 pF, and EPR₂ 16.22 k Ω .

DM inductance (leakage of two windings): L_{DM} 8.76 μ H.

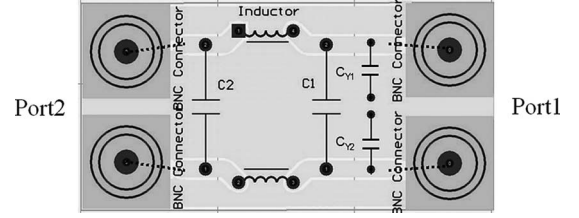


Fig. 11. PCB layout of the investigated EMI filter.

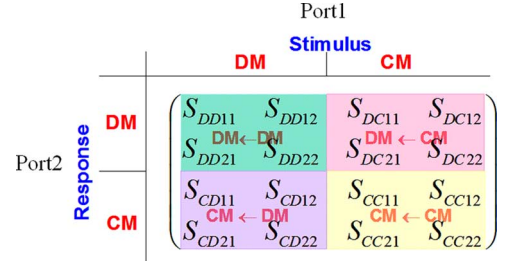


Fig. 12. Mixed-mode S parameters.

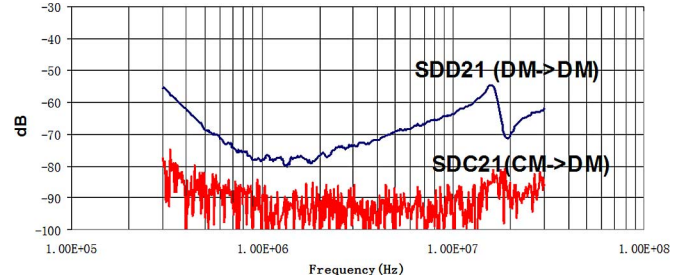


Fig. 13. Measured S parameters.

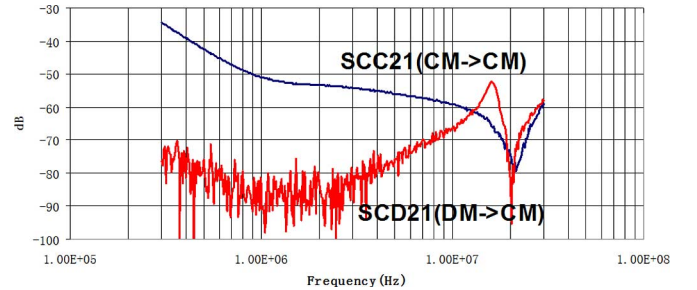


Fig. 14. Measured S parameters.

The PCB layout of the investigated EMI filter is shown in Fig. 11. The mixed-mode S parameters [2], [10] shown in Fig. 12 are used to characterize the mode transformation of the investigated EMI filter. Four parameters, S_{DD21} , S_{CC21} , S_{DC21} , and S_{CD21} are measured. They characterize the attenuations of the DM filter and the CM filter, and the transformations from CM to DM and from DM to CM, respectively.

The measurement is carried out with an Agilent E5070B four-port network analyzer [1]. Both DM and CM source impedances are set to 50 Ω . Both DM and CM load impedances are also set to 50 Ω . Measured S_{DD21} , S_{CC21} , S_{DC21} , and S_{CD21} of the filter shown in Fig. 11 are shown in Figs. 13 and 14. The noise at around -90 dB is the background noise floor

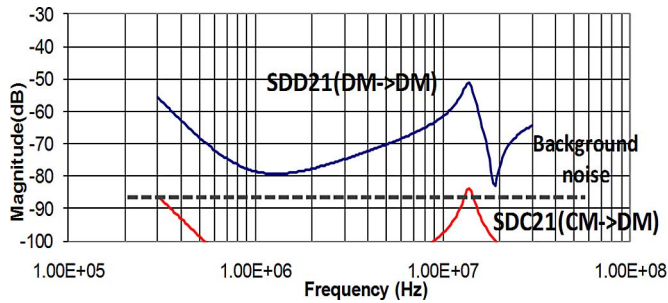


Fig. 15. Calculated curves based on extracted parameters.

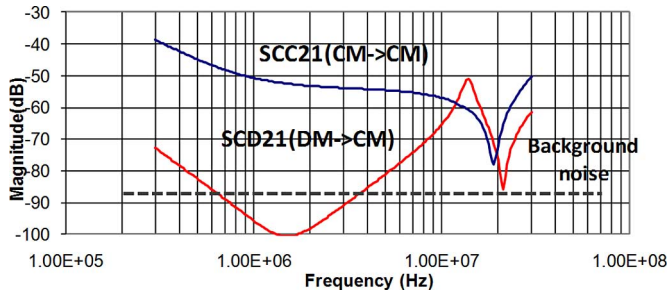


Fig. 16. Calculated curves based on extracted parameters.

of the network analyzer. The calculated (simulated in PSPICE) S_{DC21} and S_{CD21} are shown in Figs. 15 and 16. The corresponding background noise floor of the network analyzer is also shown in the figures. It should be pointed out that (37) and (38) are transfer gains, which are defined differently from S parameters, S_{DC21} and S_{CD21} . However, (37) and (38) can be used to analyze the effects of unbalance on mode transformations. Calculated S_{DD21} and S_{CC21} are also shown in Figs. 15 and 16, respectively. The effects of parasitic couplings, such as the couplings between DM inductors and DM capacitors, which are not included in previous analysis, are also included in the curves using the parasitic extraction techniques proposed in [9]. The calculated curves match measured curves. As analyzed in the last section for the effects of C_1 and C_2 , the transformation from DM to CM is more significant than the transformation from CM to DM.

In Fig. 14, the transformation from DM to CM is more significant at high frequencies than at low frequencies. Based on (37), both the unbalance of CM capacitance and DM inductance contribute to the mode transformation, and the transformation is proportional to the unbalance of the impedances of CM capacitors and DM inductors. At high frequencies, the ESL of CM capacitors C_{Y1} and C_{Y2} , and the EPC of DM inductors L_{DM1} and L_{DM2} , are dominant in the impedances of CM capacitors and DM inductors, respectively, so the unbalances of these parasitic parameters would contribute to the transformation from DM to CM at high frequencies. At low frequencies, the unbalance of the capacitance of CM capacitors and the unbalance of the inductance of DM inductors determine the transformation from DM to CM. It should be pointed out that the coefficients in (37) and (38) are the functions of frequencies. As an example, in (37), at high frequencies, k_2 and k_3 are increase when frequency increases because the impedances of capacitors increases due to

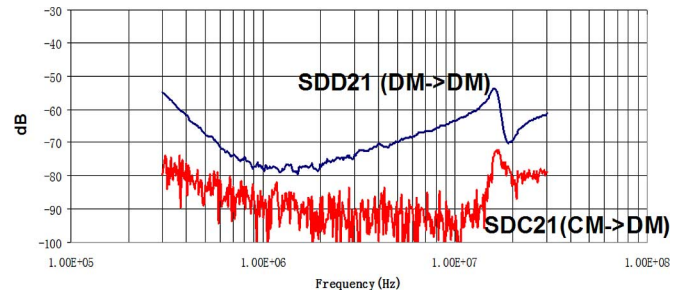
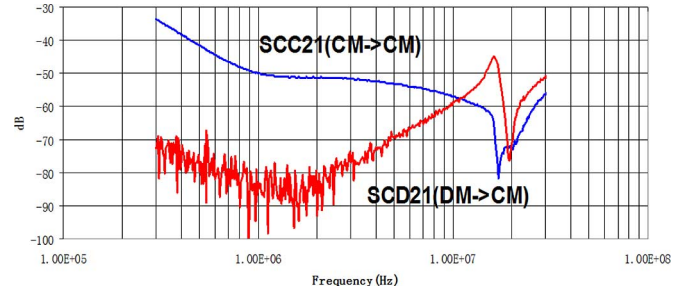
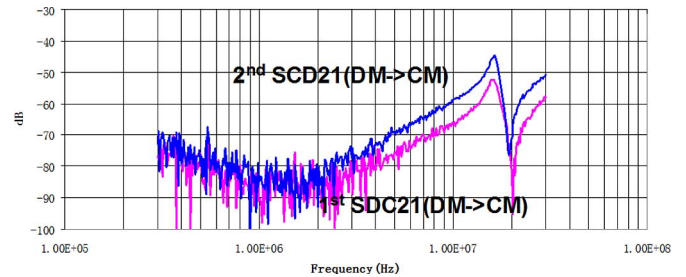
Fig. 17. Measured S parameters.Fig. 18. Measured S parameters.

Fig. 19. Comparison of transformations from DM to CM.

ESL, and the impedance of inductors decreases due to EPC, as shown in (21) and (22). This amplifies the unbalance effects of DM inductance and CM capacitance at high frequencies.

A. Effects of the Unbalance of CM Capacitors

The second experiment is carried out by changing the lead length of the two CM capacitors. For C_{Y1} , the lengths of both leads are decreased by around 1.5 mm. The measured ESL is decreased by around 2 nH. For C_{Y2} , the lengths of both leads are increased by around 1.5 mm. The measured ESL is increased by around 2 nH. Measured S_{DD21} , S_{CC21} , S_{DC21} , and S_{CD21} for the second experiment are shown in Figs. 17 and 18. The comparison of S_{CD21} in two experiments is shown in Fig. 19.

In Fig. 17, the transformation from CM to DM is still negligible compared with the transformation from DM to CM. Despite these, it is still larger than in the first experiment due to the larger unbalance between the two CM capacitors. The transformation from DM to CM becomes more significant than that in the first experiment from 2 MHz and exceeds the attenuated CM noise above 11 MHz. The comparison shown in Fig. 19 shows that a small difference between lead lengths of two CM capacitors may cause significant mode transformation at high frequencies.

Again, the measurements verified the analysis at the end of the Section II that the transformation from DM to CM is more significant than the transformation from CM to DM.

B. Effects of the Unbalance of Inductors

In order to investigate the effects of the unbalanced impedances of inductors, one winding is kept at 21 turns and the other is changed to 22 turns. The CM capacitors are kept at their original status as in the first experiment. The parameters for the two windings are as follows.

Winding 1: L_{CM1} 3.1 mH, EPC_1 6.23 pF, and EPR_1 16.22 k Ω .

Winding 2: L_{CM2} 3.4 mH, EPC_2 10.16 pF, and EPR_2 14.3 k Ω .

Total parameters of two DM inductors: 20.1 μ H, EPC 12.3 pF, and EPR 4.78 k Ω .

Based on the analysis shown in Fig. 6, the DM inductance difference ΔL_{DM} of two DM inductances is equal to the CM inductance difference ΔL_{CM} of two CM inductances, as shown in the following equation:

$$\left. \begin{aligned} L_{DM1} &= L_1 - M \\ L_{DM2} &= L_2 - M \\ L_{CM1} &= L_1 + M \\ L_{CM2} &= L_2 + M \end{aligned} \right\} \begin{aligned} \Delta L_{DM} &= \frac{L_{DM2} - L_{DM1}}{2} \\ \Delta L_{CM} &= \frac{L_{CM2} - L_{CM1}}{2} \end{aligned} \left. \vphantom{\begin{aligned} L_{DM1} \\ L_{DM2} \\ L_{CM1} \\ L_{CM2} \end{aligned}} \right\} \Delta L_{DM} \\ &= \Delta L_{CM} = \Delta L = \frac{L_2 - L_1}{2}. \quad (41)$$

Some conclusions can be drawn from (41) as follows.

- 1) The differences of CM and DM inductances are the same.
- 2) The unbalances have nothing to do with the mutual inductance M .
- 3) In the case that mutual inductance M is larger than L_1 or L_2 , L_{DM1} or L_{DM2} would be negative. For example, when $L_2 > M > L_1$, $L_{DM1} < 0$.
- 4) ΔL_{DM} can be larger than $L_{DM1} + L_{DM2}$.

The unbalance of the impedances of DM inductors before their self-resonant frequency f_{rd} can be expressed as

$$\left| \frac{\Delta Z_{LDM}}{Z_{LDM}} \right| = \left| \frac{\Delta L}{L_{DM}} \right| = \left| \frac{150 \mu\text{H}}{10.05 \mu\text{H}} \right| = 14.9, \quad \text{if } f < f_{rd}. \quad (42)$$

The unbalance of the CM inductors before the self-resonant frequency f_{rc} of the CM inductors can therefore be expressed as

$$\begin{aligned} \left| \frac{\Delta Z_{LCM}}{Z_{LCM} + Z_{Load}} \right| &= \left| \frac{\Delta L}{L_{CM} + Z_L/(2\pi f)} \right| \\ &= \left| \frac{150 \mu\text{H}}{3250 \mu\text{H} + 50\Omega/(2\pi f)} \right| \\ &\approx 0.046, \quad 150 \text{ kHz} < f < f_{rc}. \quad (43) \end{aligned}$$

Although the impedance unbalance of the CM inductors is much smaller than that of DM inductors, the coefficients of the unbalances are different, so they are not comparable. Experiments show that, for a CM unbalance, even 0.046 is a significant value. For a DM unbalance, 14.9 is also a significant value. The mode transformation below the inductor's self-resonant frequency is caused by the unbalance of CM or DM inductance. Near the DM or CM inductor's

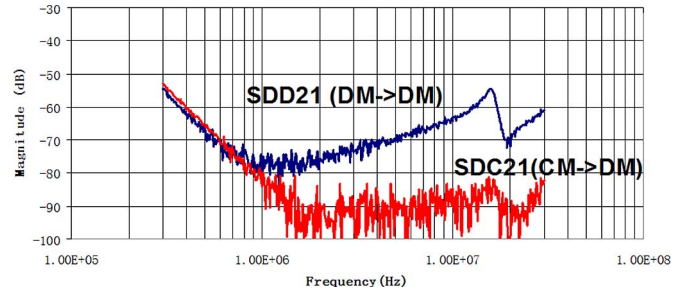


Fig. 20. Measured S parameters.

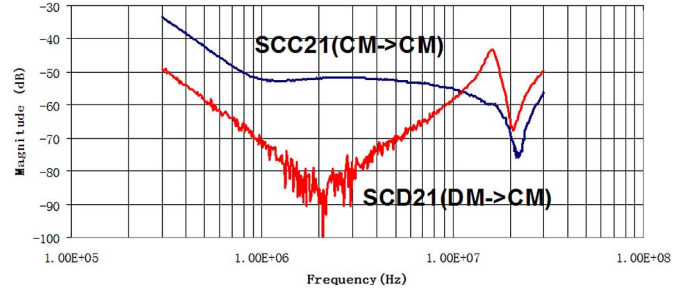


Fig. 21. Measured S parameters.

self-resonant frequency, the EPR and the quality coefficient Q determine the unbalance and mode transformation. Above the self-resonant frequency, EPC determines the unbalance and mode transformation.

When one winding is increased to 22 turns and the other is kept at 21 turns, both CM and DM inductors are unbalanced. Besides DM and CM inductances, the unbalanced parameters include the EPC and EPR of the CM and DM inductors. The measured mode transformations result from both the unbalances of CM and DM inductors.

The measurement results are shown in Figs. 20 and 21. Fig. 20 shows the mode transformation from CM to DM. In low-frequency range, the unbalance of the CM inductance causes significant transformation from CM to DM, which is even higher than the attenuated DM noise. In high-frequency range, the mode transformation is caused by EPC_{CM} , whose effects are insignificant. In Fig. 21, the mode transformation from DM to CM is significant in most of the concerned frequency range. This is caused by the unbalances of the DM inductances and EPC_{DM} .

For a practical EMI filter with the same structure shown in Fig. 1, two windings would not have different number of turns, so the mode transformation may not be as significant as shown in Figs. 20 and 21. However, when a single-ended inductor is used as a filter component, the unbalances are maximized and the aforementioned analysis applies.

IV. APPLICATION TO A PRACTICAL EMI FILTER IN POWER ELECTRONICS CIRCUITS

In this section, an EMI filter in a commercial power electronics product will be checked using the theory developed in this paper. It will be shown that after improving the balance of the

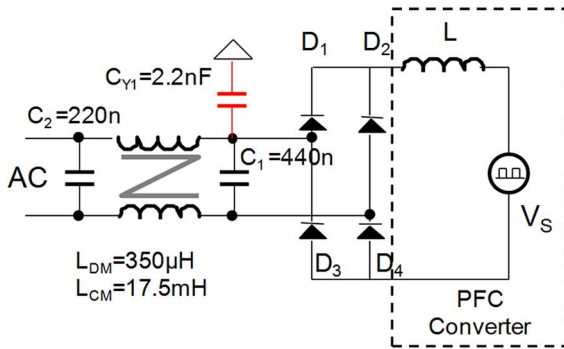


Fig. 22. EMI filter before a PFC converter.

EMI filter, the measured high-frequency CM noise is greatly reduced.

Fig. 22 shows the schematic of an EMI filter with an asymmetric structure in a commercial power electronics product. The product includes an EMI filter and a 20-W switching-mode power factor correction (PFC) converter. The EMI filter is connected to AC power lines. The PFC converter is a single-ended structure, so the noise source impedance is heavily unbalanced, as shown in the figure. On the other hand, there is no any heat sink attached to power devices, so it has a very small CM parasitic capacitance between switching devices and the ground. Because of this, ideally, there is no CM noise path in the system. So its CM noise should be very small although the noise source is unbalanced. However, it will be shown that the unbalanced filter structure will cause a high measured CM noise. On the basis of the analysis in Section II, the CM noise can be transformed from DM noise because of the unbalanced noise source impedance, unbalanced CM capacitance, or unbalanced DM inductance. For this case, both the CM capacitance and the noise source impedance are unbalanced. The unbalance $|\Delta Z_{CY}/Z_{CY}|$ is equal to 1. Equation (37) may not be directly used to analyze the transformation because (37) is derived by ignoring all second-order terms. In this case, both noise source impedance and the CM capacitance are heavily unbalanced, so the second-order terms, the product of the impedance difference of CM capacitance, and the impedance difference of noise source impedance cannot be ignored. However, the effects of unbalanced CM capacitance on the mode transformation can still be verified in experiments. Because the DM noise source is high (high-voltage switching waveforms), the transformed CM noise from DM noise can be higher than the attenuated DM noise with the filter since they flow through different paths. It is found that the unbalanced inductive couplings between the inductor L of noise source and the CM capacitor in the filter may also contribute to mode transformations.

The EMI filter is improved by balancing CM capacitor impedances and the couplings between the noise source and two CM capacitors shown in Fig. 23. Each CM capacitor has a capacitance equal to around half of the original CM capacitance. The CM noise is measured with line impedance stabilization networks (LISNs) inserted between the EMI filter and the power lines. The DM and CM noises are measured separately via a

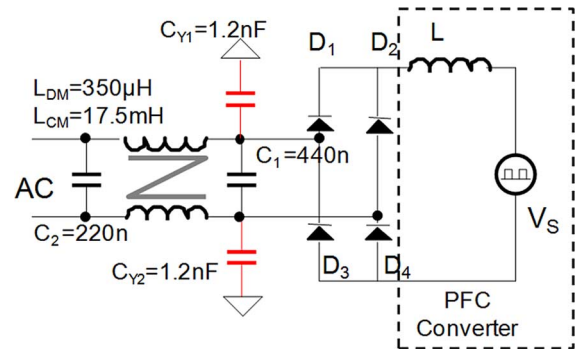


Fig. 23. Balanced filter structure.

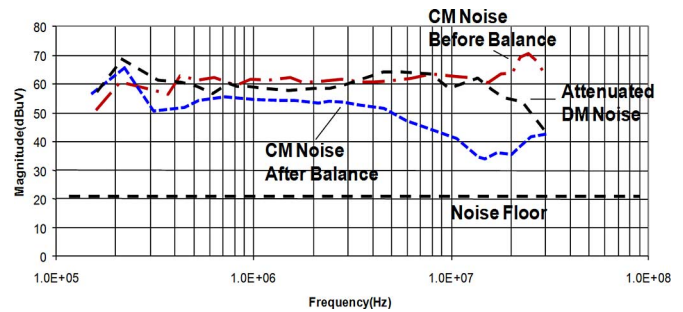


Fig. 24. Comparison of measured noise before and after balance.

noise separator [3]. The envelopes of the measured CM noise curves before and after using the balanced CM capacitors are shown in Fig. 24. Up to 30 dB, noise reduction is achieved from 300 kHz to 30 MHz after using the balanced CM capacitors. It indicates that the original filter design in the product can be further improved. It is therefore possible to reduce the sizes of CM inductors or capacitors to improve system's power density. Fig. 24 also shows the envelope of the attenuated DM noise measured on LISNs. The DM noise is almost unchanged before and after the CM capacitance is balanced, so only one DM noise envelope is shown in the figure. It is also shown that the CM noise transformed from DM noise before balance is even higher than the attenuated DM noise at high frequencies. As analyzed at the end of previous paragraph, since the original DM noise source is very high, the transformed CM noise can be higher than the attenuated DM noise at high frequencies.

The balance concept can be further generalized and used to suppress CM noise in power electronics systems. A generalized balance technique is proposed in [11] to suppress CM noise in power electronics systems. In this generalized balance concept, impedance ratio instead of symmetry is necessary to achieve a balance and noise reduction.

V. SUMMARY

This paper first analyzes the effects of unbalanced parameters in EMI filters on mode transformations. It is found that the mode transformations have a linear relationship with the unbalances of the parameters. The transformed noise due to the unbalances of CM capacitors, CM inductors and DM inductors can be higher than the attenuated noise, which makes filter

design inefficient at certain frequencies. The transformation from DM to CM would be more difficult to suppress than that from CM to DM. Experiments are then carried out to prove the analytical results. An EMI filter in a practical commercial product is finally improved using the theory.

REFERENCES

- [1] *Agilent E5070B/E5071B ENA Series RF Network Analyzers User's Guide*, 5th ed., Agilent Technologies, Santa Clara, CA, 2004, 2010.
- [2] W. Fan, A. Lu, L. L. Wai, and B. K. Lok, "Mixed-mode S-parameters characterization of differential structures," in *Proc. IEEE Electron. Packag. Technol. Conf.*, Dec., 2003, pp. 533–537.
- [3] S. Wang, F. C. Lee, and W. G. Odendaal, "Characterization, evaluation and design of noise separator for conducted EMI noise diagnosis," *IEEE Trans. Power Electron.*, vol. 20, no. 4, pp. 974–982, Jul. 2005.
- [4] R. E. Collin, *Foundations for Microwave Engineering*, 2nd ed. New York: McGraw-Hill, 1992.
- [5] R. L. Ozenbaugh, *EMI Filter Design*, 2nd ed. New York: Marcel Dekker, 2001.
- [6] M. J. Nave, *Power Line Filter Design for Switched-Mode Power Supply*. New York: Van Nostrand Reinhold, 1991.
- [7] H. W. Ott, *Noise Reduction Techniques in Electronic Systems*, 2nd ed. New York: Wiley, 1988.
- [8] S. Qu and D. Chen, "Mixed-mode EMI noise and its implications to filter design in offline switching power supplies," *IEEE Trans. Power Electron.*, vol. 17, no. 4, pp. 502–507, Jul. 2002.
- [9] S. Wang, F. C. Lee, and W. G. Odendaal, "Characterization and parasitic extraction of EMI filters using scattering parameters," *IEEE Trans. Power Electron.*, vol. 20, no. 2, pp. 502–510, Mar. 2005.
- [10] D. E. Bockelman and W. R. Eisenstadt, "Combined differential and common-mode scattering parameters: Theory and simulation," *IEEE Trans. Microw. Theory Tech.*, vol. 43, no. 7, pp. 1530–1539, Jul. 1995.
- [11] S. Wang, P. Kong, and F. C. Lee, "Common mode noise reduction for boost converters using general balance technique," *IEEE Trans. Power Electron.*, vol. 22, no. 4, pp. 1410–1416, Jul. 2007.



Shuo Wang (S'03–M'06–SM'07) received the B.S.E.E. degree from Southwest Jiaotong University, Chengdu, China, in 1994, the M.S.E.E. degree from Zhejiang University, Hangzhou, China, in 1997, and the Ph.D. degree from the Center for Power Electronics Systems, Virginia Polytechnic Institute and State University (Virginia Tech), Blacksburg, in 2005.

From 2005 to 2009, he was a Research Assistant Professor at the Center for Power Electronics Systems, Virginia Tech. Since 2009, he has been with Electrical Power Systems, GE Aviation Systems, Vandalia, OH. He holds four U.S. patents and two pending patents. He has authored and coauthored more than 70 academic papers published in the IEEE Transactions and IEEE conferences. His current research interests include electromagnetic interference/electromagnetic compatibility in power electronics systems, high-density power conversion, three-phase power conversion and inversion, motor drive, generator control, and power systems.

Dr. Wang is an Associate Editor for the IEEE TRANSACTIONS ON INDUSTRY APPLICATIONS. He was the recipient of the 2005 Best Transaction Paper Award from the IEEE TRANSACTIONS ON POWER ELECTRONICS and the William M. Portnoy Award for the best paper published in the IEEE Industry Applications Society Annual Conference in 2004.



Fred C. Lee (S'72–M'74–SM'87–F'90) received the B.S. degree in electrical engineering from the National Cheng Kung University, Tainan, Taiwan, in 1968, and the M.S. and Ph.D. degrees in electrical engineering from Duke University, Durham, NC, in 1972 and 1974, respectively.

He is currently a University Distinguished Professor at Virginia Polytechnic Institute and State University, Blacksburg, where he is the Director of the Center for Power Electronics Systems, a National Science Foundation Engineering Research Center whose

participants include five universities and more than 80 corporations. He holds 30 U.S. patents. He is the author or coauthor of more than 175 journal articles in refereed journals and more than 400 technical papers in conference proceedings.

Prof. Lee was a recipient of the Society of Automotive Engineering's Ralph R. Teeter Education Award (1985), Virginia Tech's Alumni Award for Research Excellence (1990), and Virginia Tech's College of Engineering Dean's Award for Excellence in Research (1997). He was the recipient of the 1989 William E. Newell Power Electronics Award, the highest award presented by the IEEE Power Electronics Society for outstanding achievement in the power electronics discipline. He was also the recipient of the Power Conversion and Intelligent Motion Award for Leadership in Power Electronics Education (1990), the Arthur E. Fury Award for Leadership and Innovation in Advancing Power Electronic Systems Technology (1998), and the IEEE Millennium Medal.